

# Amplitude Analysis of Singly Cabibbo-Suppressed Decay $\Lambda_c^+ \rightarrow pK^+K^-$

M. Ablikim<sup>1</sup>, M. N. Achasov<sup>4,c</sup>, P. Adlarson<sup>82</sup>, X. C. Ai<sup>87</sup>, R. Aliberti<sup>39</sup>, A. Amoroso<sup>81A,81C</sup>, Q. An<sup>78,64,†</sup>,  
 Y. Bai<sup>62</sup>, O. Bakina<sup>40</sup>, Y. Ban<sup>50,h</sup>, H.-R. Bao<sup>70</sup>, V. Batotzkaya<sup>1,48</sup>, K. Begzsuren<sup>35</sup>, N. Berger<sup>39</sup>,  
 M. Berlowski<sup>48</sup>, M. B. Bertani<sup>30A</sup>, D. Bettoni<sup>31A</sup>, F. Bianchi<sup>81A,81C</sup>, E. Bianco<sup>81A,81C</sup>, A. Bortone<sup>81A,81C</sup>,  
 I. Boyko<sup>40</sup>, R. A. Briere<sup>5</sup>, A. Brueggemann<sup>75</sup>, H. Cai<sup>83</sup>, M. H. Cai<sup>42,k,l</sup>, X. Cai<sup>1,64</sup>, A. Calcaterra<sup>30A</sup>,  
 G. F. Cao<sup>1,70</sup>, N. Cao<sup>1,70</sup>, S. A. Cetin<sup>68A</sup>, X. Y. Chai<sup>50,h</sup>, J. F. Chang<sup>1,64</sup>, T. T. Chang<sup>47</sup>, G. R. Che<sup>47</sup>,  
 Y. Z. Che<sup>1,64,70</sup>, C. H. Chen<sup>10</sup>, Chao Chen<sup>60</sup>, G. Chen<sup>1</sup>, H. S. Chen<sup>1,70</sup>, H. Y. Chen<sup>21</sup>, M. L. Chen<sup>1,64,70</sup>,  
 S. J. Chen<sup>46</sup>, S. M. Chen<sup>67</sup>, T. Chen<sup>1,70</sup>, X. R. Chen<sup>34,70</sup>, X. T. Chen<sup>1,70</sup>, X. Y. Chen<sup>12,g</sup>, Y. B. Chen<sup>1,64</sup>,  
 Y. Q. Chen<sup>16</sup>, Z. K. Chen<sup>65</sup>, J. C. Cheng<sup>49</sup>, L. N. Cheng<sup>47</sup>, S. K. Choi<sup>11</sup>, X. Chu<sup>12,g</sup>, G. Cibinetto<sup>31A</sup>,  
 F. Cossio<sup>81C</sup>, J. Cottee-Meldrum<sup>69</sup>, H. L. Dai<sup>1,64</sup>, J. P. Dai<sup>85</sup>, X. C. Dai<sup>67</sup>, A. Dbeysi<sup>19</sup>, R. E. de Boer<sup>3</sup>,  
 D. Dedovich<sup>40</sup>, C. Q. Deng<sup>79</sup>, Z. Y. Deng<sup>1</sup>, A. Denig<sup>39</sup>, I. Denisenko<sup>40</sup>, M. Destefanis<sup>81A,81C</sup>,  
 F. De Mori<sup>81A,81C</sup>, X. X. Ding<sup>50,h</sup>, Y. Ding<sup>44</sup>, Y. X. Ding<sup>32</sup>, J. Dong<sup>1,64</sup>, L. Y. Dong<sup>1,70</sup>, M. Y. Dong<sup>1,64,70</sup>,  
 X. Dong<sup>83</sup>, M. C. Du<sup>1</sup>, S. X. Du<sup>87</sup>, S. X. Du<sup>12,g</sup>, X. L. Du<sup>87</sup>, Y. Y. Duan<sup>60</sup>, Z. H. Duan<sup>46</sup>, P. Egorov<sup>40,b</sup>,  
 G. F. Fan<sup>46</sup>, J. J. Fan<sup>20</sup>, Y. H. Fan<sup>49</sup>, J. Fang<sup>1,64</sup>, J. Fang<sup>65</sup>, S. S. Fang<sup>1,70</sup>, W. X. Fang<sup>1</sup>,  
 Y. Q. Fang<sup>1,64,†</sup>, L. Fava<sup>81B,81C</sup>, F. Feldbauer<sup>3</sup>, G. Felici<sup>30A</sup>, C. Q. Feng<sup>78,64</sup>, J. H. Feng<sup>16</sup>, L. Feng<sup>42,k,l</sup>,  
 Q. X. Feng<sup>42,k,l</sup>, Y. T. Feng<sup>78,64</sup>, M. Fritsch<sup>3</sup>, C. D. Fu<sup>1</sup>, J. L. Fu<sup>70</sup>, Y. W. Fu<sup>1,70</sup>, H. Gao<sup>70</sup>, Y. Gao<sup>78,64</sup>,  
 Y. N. Gao<sup>50,h</sup>, Y. N. Gao<sup>20</sup>, Y. Y. Gao<sup>32</sup>, Z. Gao<sup>47</sup>, S. Garbolino<sup>81C</sup>, I. Garzia<sup>31A,31B</sup>, L. Ge<sup>62</sup>,  
 P. T. Ge<sup>20</sup>, Z. W. Ge<sup>46</sup>, C. Geng<sup>65</sup>, E. M. Gersabeck<sup>74</sup>, A. Gilman<sup>76</sup>, K. Goetzen<sup>13</sup>, J. D. Gong<sup>38</sup>,  
 L. Gong<sup>44</sup>, W. X. Gong<sup>1,64</sup>, W. Gradl<sup>39</sup>, S. Gramigna<sup>31A,31B</sup>, M. Greco<sup>81A,81C</sup>, M. D. Gu<sup>55</sup>, M. H. Gu<sup>1,64</sup>,  
 C. Y. Guan<sup>1,70</sup>, A. Q. Guo<sup>34</sup>, J. N. Guo<sup>12,g</sup>, L. B. Guo<sup>45</sup>, M. J. Guo<sup>54</sup>, R. P. Guo<sup>53</sup>, X. Guo<sup>54</sup>,  
 Y. P. Guo<sup>12,g</sup>, A. Guskov<sup>40,b</sup>, J. Gutierrez<sup>29</sup>, T. T. Han<sup>1</sup>, F. Hanisch<sup>3</sup>, K. D. Hao<sup>78,64</sup>, X. Q. Hao<sup>20</sup>,  
 F. A. Harris<sup>72</sup>, C. Z. He<sup>50,h</sup>, K. L. He<sup>1,70</sup>, F. H. Heinsius<sup>3</sup>, C. H. Heinz<sup>39</sup>, Y. K. Heng<sup>1,64,70</sup>, C. Herold<sup>66</sup>,  
 P. C. Hong<sup>38</sup>, G. Y. Hou<sup>12,g</sup>, X. T. Hou<sup>1,70</sup>, Y. R. Hou<sup>70</sup>, Z. L. Hou<sup>1</sup>, H. M. Hu<sup>1,70</sup>, J. F. Hu<sup>61,j</sup>,  
 Q. P. Hu<sup>78,64</sup>, S. L. Hu<sup>12,g</sup>, T. Hu<sup>1,64,70</sup>, Y. Hu<sup>1</sup>, Z. M. Hu<sup>65</sup>, G. S. Huang<sup>78,64</sup>, K. X. Huang<sup>65</sup>,  
 L. Q. Huang<sup>34,70</sup>, P. Huang<sup>46</sup>, X. T. Huang<sup>54</sup>, Y. P. Huang<sup>1</sup>, Y. S. Huang<sup>65</sup>, T. Hussain<sup>65</sup>, N. Hüsken<sup>39</sup>,  
 N. in der Wiesche<sup>75</sup>, J. Jackson<sup>29</sup>, Q. Ji<sup>1</sup>, Q. P. Ji<sup>20</sup>, W. Ji<sup>1,70</sup>, X. B. Ji<sup>1,70</sup>, X. L. Ji<sup>1,64</sup>, X. Q. Jia<sup>54</sup>,  
 Z. K. Jia<sup>78,64</sup>, D. Jiang<sup>1,70</sup>, H. B. Jiang<sup>83</sup>, P. C. Jiang<sup>50,h</sup>, S. J. Jiang<sup>10</sup>, X. S. Jiang<sup>1,64,70</sup>, Y. Jiang<sup>70</sup>,  
 J. B. Jiao<sup>54</sup>, J. K. Jiao<sup>38</sup>, Z. Jiao<sup>25</sup>, S. Jin<sup>46</sup>, Y. Jin<sup>73</sup>, M. Q. Jing<sup>1,70</sup>, X. M. Jing<sup>70</sup>, T. Johansson<sup>82</sup>,  
 S. Kabana<sup>36</sup>, N. Kalantar-Nayestanaki<sup>71</sup>, X. L. Kang<sup>10</sup>, X. S. Kang<sup>44</sup>, M. Kavatsyuk<sup>71</sup>, B. C. Ke<sup>87</sup>,  
 V. Khachatryan<sup>29</sup>, A. Khoukaz<sup>75</sup>, O. B. Kolcu<sup>68A</sup>, B. Kopf<sup>63</sup>, L. Kröger<sup>75</sup>, M. Kuessner<sup>3</sup>, X. Kui<sup>1,70</sup>,  
 N. Kumar<sup>28</sup>, A. Kupcs<sup>48,82</sup>, W. Kühn<sup>41</sup>, Q. Lan<sup>79</sup>, W. N. Lan<sup>20</sup>, T. T. Lei<sup>78,64</sup>, M. Lellmann<sup>39</sup>,  
 T. Lenz<sup>39</sup>, C. Li<sup>51</sup>, C. Li<sup>47</sup>, C. H. Li<sup>45</sup>, C. K. Li<sup>21</sup>, D. M. Li<sup>87</sup>, F. Li<sup>1,64</sup>, G. Li<sup>1</sup>, H. B. Li<sup>1,70</sup>,  
 H. J. Li<sup>20</sup>, H. L. Li<sup>87</sup>, H. N. Li<sup>61,j</sup>, Hui Li<sup>47</sup>, J. R. Li<sup>67</sup>, J. S. Li<sup>65</sup>, J. W. Li<sup>54</sup>, K. Li<sup>1</sup>, K. L. Li<sup>42,k,l</sup>,  
 L. J. Li<sup>1,70</sup>, Lei Li<sup>52</sup>, M. H. Li<sup>47</sup>, M. R. Li<sup>1,70</sup>, P. L. Li<sup>70</sup>, P. R. Li<sup>42,k,l</sup>, Q. M. Li<sup>1,70</sup>, Q. X. Li<sup>54</sup>,  
 R. Li<sup>18,34</sup>, S. X. Li<sup>12</sup>, Shanshan Li<sup>27,i</sup>, T. Li<sup>54</sup>, T. Y. Li<sup>47</sup>, W. D. Li<sup>1,70</sup>, W. G. Li<sup>1,i</sup>, X. Li<sup>1,70</sup>,  
 X. H. Li<sup>78,64</sup>, X. K. Li<sup>50,h</sup>, X. L. Li<sup>54</sup>, X. Y. Li<sup>1,9</sup>, X. Z. Li<sup>65</sup>, Y. Li<sup>20</sup>, Y. G. Li<sup>50,h</sup>, Y. P. Li<sup>38</sup>,  
 Z. H. Li<sup>42</sup>, Z. J. Li<sup>65</sup>, Z. X. Li<sup>47</sup>, Z. Y. Li<sup>85</sup>, C. Liang<sup>46</sup>, H. Liang<sup>78,64</sup>, Y. F. Liang<sup>59</sup>, Y. T. Liang<sup>34,70</sup>,  
 G. R. Liao<sup>14</sup>, L. B. Liao<sup>65</sup>, M. H. Liao<sup>65</sup>, Y. P. Liao<sup>1,70</sup>, J. Libby<sup>28</sup>, A. Limphirat<sup>66</sup>, D. X. Liu<sup>34,70</sup>,  
 L. Q. Lin<sup>43</sup>, T. Lin<sup>1</sup>, B. J. Liu<sup>1</sup>, B. X. Liu<sup>83</sup>, C. X. Liu<sup>1</sup>, F. Liu<sup>1</sup>, F. H. Liu<sup>58</sup>, Feng Liu<sup>6</sup>, G. M. Liu<sup>61,j</sup>,  
 H. Liu<sup>42,k,l</sup>, H. B. Liu<sup>15</sup>, H. M. Liu<sup>1,70</sup>, Huihui Liu<sup>22</sup>, J. B. Liu<sup>78,64</sup>, J. J. Liu<sup>21</sup>, K. Liu<sup>42,k,l</sup>, K. Liu<sup>79</sup>,  
 K. Y. Liu<sup>44</sup>, Ke Liu<sup>23</sup>, L. Liu<sup>42</sup>, L. C. Liu<sup>47</sup>, Lu Liu<sup>47</sup>, M. H. Liu<sup>38</sup>, P. L. Liu<sup>1</sup>, Q. Liu<sup>70</sup>, S. B. Liu<sup>78,64</sup>,  
 W. M. Liu<sup>78,64</sup>, W. T. Liu<sup>43</sup>, X. Liu<sup>42,k,l</sup>, X. K. Liu<sup>42,k,l</sup>, X. L. Liu<sup>12,g</sup>, X. Y. Liu<sup>83</sup>, Y. Liu<sup>42,k,l</sup>, Y. Liu<sup>87</sup>,  
 Y. B. Liu<sup>47</sup>, Z. A. Liu<sup>1,64,70</sup>, Z. D. Liu<sup>10</sup>, Z. Q. Liu<sup>54</sup>, Z. Y. Liu<sup>42</sup>, X. C. Lou<sup>1,64,70</sup>, H. J. Lu<sup>25</sup>,  
 J. G. Lu<sup>1,64</sup>, X. L. Lu<sup>16</sup>, Y. Lu<sup>7</sup>, Y. H. Lu<sup>1,70</sup>, Y. P. Lu<sup>1,64</sup>, Z. H. Lu<sup>1,70</sup>, C. L. Luo<sup>45</sup>, J. R. Luo<sup>65</sup>,  
 J. S. Luo<sup>1,70</sup>, M. X. Luo<sup>86</sup>, T. Luo<sup>12,g</sup>, X. L. Luo<sup>1,64</sup>, Z. Y. Lv<sup>23</sup>, X. R. Lyu<sup>70,o</sup>, Y. F. Lyu<sup>47</sup>, Y. H. Lyu<sup>87</sup>,  
 F. C. Ma<sup>44</sup>, H. L. Ma<sup>1</sup>, Heng Ma<sup>27,i</sup>, J. L. Ma<sup>1,70</sup>, L. L. Ma<sup>54</sup>, L. R. Ma<sup>73</sup>, Q. M. Ma<sup>1</sup>, R. Q. Ma<sup>1,70</sup>,  
 R. Y. Ma<sup>20</sup>, T. Ma<sup>78,64</sup>, X. T. Ma<sup>1,70</sup>, X. Y. Ma<sup>1,64</sup>, Y. M. Ma<sup>34</sup>, F. E. Maas<sup>19</sup>, I. MacKay<sup>76</sup>,  
 M. Maggiora<sup>81A,81C</sup>, S. Malde<sup>76</sup>, Q. A. Malik<sup>80</sup>, H. X. Mao<sup>42,k,l</sup>, Y. J. Mao<sup>50,h</sup>, Z. P. Mao<sup>1</sup>,  
 S. Marcello<sup>81A,81C</sup>, A. Marshall<sup>69</sup>, F. M. Melendi<sup>31A,31B</sup>, Y. H. Meng<sup>70</sup>, Z. X. Meng<sup>73</sup>, G. Mezzadri<sup>31A</sup>,  
 H. Miao<sup>1,70</sup>, T. J. Min<sup>46</sup>, R. E. Mitchell<sup>29</sup>, X. H. Mo<sup>1,64,70</sup>, B. Moses<sup>29</sup>, N. Yu. Muchnoi<sup>4,c</sup>, J. Muskalla<sup>39</sup>,  
 Y. Nefedov<sup>40</sup>, F. Nerling<sup>19,e</sup>, H. Neuwirth<sup>75</sup>, Z. Ning<sup>1,64</sup>, S. Nisar<sup>33,a</sup>, Q. L. Niu<sup>42,k,l</sup>, W. D. Niu<sup>12,g</sup>,  
 Y. Niu<sup>54</sup>, C. Normand<sup>69</sup>, S. L. Olsen<sup>11,70</sup>, Q. Ouyang<sup>1,64,70</sup>, S. Pacetti<sup>30B,30C</sup>, X. Pan<sup>60</sup>, Y. Pan<sup>62</sup>,  
 A. Pathak<sup>11</sup>, Y. P. Pei<sup>78,64</sup>, M. Pelizaeus<sup>3</sup>, H. P. Peng<sup>78,64</sup>, X. J. Peng<sup>42,k,l</sup>, Y. Y. Peng<sup>42,k,l</sup>, K. Peters<sup>13,e</sup>,  
 K. Petridis<sup>69</sup>, J. L. Ping<sup>45</sup>, R. G. Ping<sup>1,70</sup>, S. Plura<sup>39</sup>, V. Prasad<sup>38</sup>, F. Z. Qi<sup>1</sup>, H. R. Qi<sup>67</sup>, M. Qi<sup>46</sup>,  
 S. Qian<sup>1,64</sup>, W. B. Qian<sup>70</sup>, C. F. Qiao<sup>70</sup>, J. H. Qiao<sup>20</sup>, J. J. Qin<sup>79</sup>, J. L. Qin<sup>60</sup>, L. Q. Qin<sup>14</sup>,  
 L. Y. Qin<sup>78,64</sup>, P. B. Qin<sup>79</sup>, X. P. Qin<sup>43</sup>, X. S. Qin<sup>54</sup>, Z. H. Qin<sup>1,64</sup>, J. F. Qiu<sup>1</sup>, Z. H. Qu<sup>79</sup>,  
 J. Rademacker<sup>69</sup>, C. F. Redmer<sup>39</sup>, A. Rivetti<sup>81C</sup>, M. Rolo<sup>81C</sup>, G. Rong<sup>1,70</sup>, S. S. Rong<sup>1,70</sup>, F. Rosini<sup>30B,30C</sup>,  
 Ch. Rosner<sup>19</sup>, M. Q. Ruan<sup>1,64</sup>, N. Salone<sup>48,p</sup>, A. Sarantsev<sup>40,d</sup>, Y. Schelhaas<sup>39</sup>, K. Schoenning<sup>82</sup>,  
 M. Scodreggio<sup>31A</sup>, W. Shan<sup>26</sup>, X. Y. Shan<sup>78,64</sup>, Z. J. Shang<sup>42,k,l</sup>, J. F. Shanguan<sup>17</sup>, L. G. Shao<sup>1,70</sup>,  
 M. Shao<sup>78,64</sup>, C. P. Shen<sup>12,g</sup>, H. F. Shen<sup>1,9</sup>, W. H. Shen<sup>70</sup>, X. Y. Shen<sup>1,70</sup>, B. A. Shi<sup>70</sup>, H. Shi<sup>78,64</sup>,  
 J. L. Shi<sup>8,q</sup>, J. Y. Shi<sup>1</sup>, S. Y. Shi<sup>79</sup>, X. Shi<sup>1,64</sup>, H. L. Song<sup>78,64</sup>, J. J. Song<sup>20</sup>, M. H. Song<sup>42</sup>, T. Z. Song<sup>65</sup>,  
 W. M. Song<sup>38</sup>, Y. X. Song<sup>50,h,m</sup>, Zirong Song<sup>27,i</sup>, S. Sosio<sup>81A,81C</sup>, S. Spataro<sup>81A,81C</sup>, S. Stanslaus<sup>76</sup>,

F. Stieler<sup>39</sup> , S. S. Su<sup>44</sup> , G. B. Sun<sup>83</sup> , G. X. Sun<sup>1</sup> , H. Sun<sup>70</sup> , H. K. Sun<sup>1</sup> , J. F. Sun<sup>20</sup> , K. Sun<sup>67</sup> , L. Sun<sup>83</sup> ,  
R. Sun<sup>78</sup> , S. S. Sun<sup>1,70</sup> , T. Sun<sup>56,f</sup> , W. Y. Sun<sup>55</sup> , Y. C. Sun<sup>83</sup> , Y. H. Sun<sup>32</sup> , Y. J. Sun<sup>78,64</sup> , Y. Z. Sun<sup>1</sup> ,  
Z. Q. Sun<sup>1</sup> , Z. T. Sun<sup>54</sup> , C. J. Tang<sup>59</sup> , G. Y. Tang<sup>1</sup> , J. Tang<sup>65</sup> , J. J. Tang<sup>78,64</sup> , L. F. Tang<sup>43</sup> ,  
Y. A. Tang<sup>83</sup> , L. Y. Tao<sup>79</sup> , M. Tat<sup>76</sup> , J. X. Teng<sup>78,64</sup> , J. Y. Tian<sup>78,64</sup> , W. H. Tian<sup>65</sup> , Y. Tian<sup>34</sup> ,  
Z. F. Tian<sup>83</sup> , I. Uman<sup>68B</sup> , B. Wang<sup>1</sup> , B. Wang<sup>65</sup> , Bo Wang<sup>78,64</sup> , C. Wang<sup>42,k,l</sup> , C. Wang<sup>20</sup> , Cong Wang<sup>23</sup> ,  
D. Y. Wang<sup>50,h</sup> , H. J. Wang<sup>42,k,l</sup> , J. Wang<sup>10</sup> , J. J. Wang<sup>83</sup> , J. P. Wang<sup>54</sup> , J. P. Wang<sup>37</sup> , K. Wang<sup>1,64</sup> ,  
L. L. Wang<sup>1</sup> , L. W. Wang<sup>38</sup> , M. Wang<sup>54</sup> , M. Wang<sup>78,64</sup> , N. Y. Wang<sup>70</sup> , S. Wang<sup>42,k,l</sup> , Shun Wang<sup>63</sup> ,  
T. Wang<sup>12,g</sup> , T. J. Wang<sup>47</sup> , W. Wang<sup>65</sup> , W. P. Wang<sup>39</sup> , X. Wang<sup>50,h</sup> , X. F. Wang<sup>42,k,l</sup> , X. L. Wang<sup>12,g</sup> ,  
X. N. Wang<sup>1,70</sup> , Xin Wang<sup>27,i</sup> , Y. Wang<sup>1</sup> , Y. D. Wang<sup>49</sup> , Y. F. Wang<sup>1,9,70</sup> , Y. H. Wang<sup>42,k,l</sup> ,  
Y. J. Wang<sup>78,64</sup> , Y. L. Wang<sup>20</sup> , Y. N. Wang<sup>49</sup> , Y. N. Wang<sup>83</sup> , Yaqian Wang<sup>18</sup> , Yi Wang<sup>67</sup> , Yuan Wang<sup>18,34</sup> ,  
Z. Wang<sup>1,64</sup> , Z. Wang<sup>47</sup> , Z. L. Wang<sup>2</sup> , Z. Q. Wang<sup>12,g</sup> , Z. Y. Wang<sup>1,70</sup> , Ziyi Wang<sup>70</sup> , D. Wei<sup>47</sup> ,  
D. H. Wei<sup>14</sup> , H. R. Wei<sup>47</sup> , F. Weidner<sup>75</sup> , S. P. Wen<sup>1</sup> , U. Wiedner<sup>3</sup> , G. Wilkinson<sup>76</sup> , M. Wolke<sup>82</sup> , J. F. Wu<sup>1,9</sup> ,  
L. H. Wu<sup>1</sup> , L. J. Wu<sup>20</sup> , Lianjie Wu<sup>20</sup> , S. G. Wu<sup>1,70</sup> , S. M. Wu<sup>70</sup> , X. W. Wu<sup>79</sup> , Y. J. Wu<sup>34</sup> , Z. Wu<sup>1,64</sup> ,  
L. Xia<sup>78,64</sup> , B. H. Xiang<sup>1,70</sup> , D. Xiao<sup>42,k,l</sup> , G. Y. Xiao<sup>46</sup> , H. Xiao<sup>79</sup> , Y. L. Xiao<sup>12,g</sup> , Z. J. Xiao<sup>45</sup> , C. Xie<sup>46</sup> ,  
K. J. Xie<sup>1,70</sup> , Y. Xie<sup>54</sup> , Y. G. Xie<sup>1,64</sup> , Y. H. Xie<sup>6</sup> , Z. P. Xie<sup>78,64</sup> , T. Y. Xing<sup>1,70</sup> , C. J. Xu<sup>65</sup> , G. F. Xu<sup>1</sup> ,  
H. Y. Xu<sup>2</sup> , M. Xu<sup>78,64</sup> , Q. J. Xu<sup>17</sup> , Q. N. Xu<sup>32</sup> , T. D. Xu<sup>79</sup> , X. P. Xu<sup>60</sup> , Y. Xu<sup>12,g</sup> , Y. C. Xu<sup>84</sup> ,  
Z. S. Xu<sup>70</sup> , F. Yan<sup>24</sup> , L. Yan<sup>12,g</sup> , W. B. Yan<sup>78,64</sup> , W. C. Yan<sup>87</sup> , W. H. Yan<sup>6</sup> , W. P. Yan<sup>20</sup> , X. Q. Yan<sup>1,70</sup> ,  
H. J. Yang<sup>56,f</sup> , H. L. Yang<sup>38</sup> , H. X. Yang<sup>1</sup> , J. H. Yang<sup>46</sup> , R. J. Yang<sup>20</sup> , Y. Yang<sup>12,g</sup> , Y. H. Yang<sup>46</sup> ,  
Y. Q. Yang<sup>10</sup> , Y. Z. Yang<sup>20</sup> , Z. P. Yao<sup>54</sup> , M. Ye<sup>1,64</sup> , M. H. Ye<sup>9,†</sup> , Z. J. Ye<sup>61,j</sup> , Junhao Yin<sup>47</sup> , Z. Y. You<sup>65</sup> ,  
B. X. Yu<sup>1,64,70</sup> , C. X. Yu<sup>47</sup> , G. Yu<sup>13</sup> , J. S. Yu<sup>27,i</sup> , L. W. Yu<sup>12,g</sup> , T. Yu<sup>79</sup> , X. D. Yu<sup>50,h</sup> , Y. C. Yu<sup>87</sup> ,  
Y. C. Yu<sup>42</sup> , C. Z. Yuan<sup>1,70</sup> , H. Yuan<sup>1,70</sup> , J. S. Yuan<sup>38</sup> , J. Yuan<sup>49</sup> , L. Yuan<sup>2</sup> , M. K. Yuan<sup>12,g</sup> , S. H. Yuan<sup>79</sup> ,  
Y. Yuan<sup>1,70</sup> , C. X. Yue<sup>43</sup> , Ying Yue<sup>20</sup> , A. A. Zafar<sup>80</sup> , F. R. Zeng<sup>54</sup> , S. H. Zeng<sup>69</sup> , X. Zeng<sup>12,g</sup> ,  
Yujie Zeng<sup>65</sup> , Y. J. Zeng<sup>1,70</sup> , Y. C. Zhai<sup>54</sup> , Y. H. Zhan<sup>65</sup> , Shunan Zhang<sup>76</sup> , B. L. Zhang<sup>1,70</sup> , B. X. Zhang<sup>1,†</sup> ,  
D. H. Zhang<sup>47</sup> , G. Y. Zhang<sup>20</sup> , G. Y. Zhang<sup>1,70</sup> , H. Zhang<sup>78,64</sup> , H. Zhang<sup>87</sup> , H. C. Zhang<sup>1,64,70</sup> ,  
H. H. Zhang<sup>65</sup> , H. Q. Zhang<sup>1,64,70</sup> , H. R. Zhang<sup>78,64</sup> , H. Y. Zhang<sup>1,64</sup> , J. Zhang<sup>65</sup> , J. J. Zhang<sup>57</sup> ,  
J. L. Zhang<sup>21</sup> , J. Q. Zhang<sup>45</sup> , J. S. Zhang<sup>12,g</sup> , J. W. Zhang<sup>1,64,70</sup> , J. X. Zhang<sup>42,k,l</sup> , J. Y. Zhang<sup>1</sup> ,  
J. Z. Zhang<sup>1,70</sup> , Jianyu Zhang<sup>70</sup> , L. M. Zhang<sup>67</sup> , Lei Zhang<sup>46</sup> , N. Zhang<sup>87</sup> , P. Zhang<sup>1,9</sup> , Q. Zhang<sup>20</sup> ,  
Q. Y. Zhang<sup>38</sup> , R. Y. Zhang<sup>42,k,l</sup> , S. H. Zhang<sup>1,70</sup> , Shulei Zhang<sup>27,i</sup> , X. M. Zhang<sup>1</sup> , X. Y. Zhang<sup>54</sup> ,  
Y. Zhang<sup>1</sup> , Y. Zhang<sup>79</sup> , Y. T. Zhang<sup>87</sup> , Y. H. Zhang<sup>1,64</sup> , Y. P. Zhang<sup>78,64</sup> , Z. D. Zhang<sup>1</sup> , Z. H. Zhang<sup>1</sup> ,  
Z. L. Zhang<sup>38</sup> , Z. L. Zhang<sup>60</sup> , Z. X. Zhang<sup>20</sup> , Z. Y. Zhang<sup>83</sup> , Z. Y. Zhang<sup>47</sup> , Z. Z. Zhang<sup>49</sup> , Zh. Zh. Zhang<sup>20</sup> ,  
G. Zhao<sup>1</sup> , J. Y. Zhao<sup>1,70</sup> , J. Z. Zhao<sup>1,64</sup> , L. Zhao<sup>1</sup> , L. Zhao<sup>78,64</sup> , M. G. Zhao<sup>47</sup> , S. J. Zhao<sup>87</sup> ,  
Y. B. Zhao<sup>1,64</sup> , Y. L. Zhao<sup>60</sup> , Y. X. Zhao<sup>34,70</sup> , Z. G. Zhao<sup>78,64</sup> , A. Zhemchugov<sup>40,b</sup> , B. Zheng<sup>79</sup> ,  
B. M. Zheng<sup>38</sup> , J. P. Zheng<sup>1,64</sup> , W. J. Zheng<sup>1,70</sup> , X. R. Zheng<sup>20</sup> , Y. H. Zheng<sup>70,o</sup> , B. Zhong<sup>45</sup> , C. Zhong<sup>20</sup> ,  
H. Zhou<sup>39,54,n</sup> , J. Q. Zhou<sup>38</sup> , S. Zhou<sup>6</sup> , X. Zhou<sup>83</sup> , X. K. Zhou<sup>6</sup> , X. R. Zhou<sup>78,64</sup> , X. Y. Zhou<sup>43</sup> ,  
Y. X. Zhou<sup>84</sup> , Y. Z. Zhou<sup>12,g</sup> , A. N. Zhu<sup>70</sup> , J. Zhu<sup>47</sup> , K. Zhu<sup>1</sup> , K. J. Zhu<sup>1,64,70</sup> , K. S. Zhu<sup>12,g</sup> ,  
L. X. Zhu<sup>70</sup> , Lin Zhu<sup>20</sup> , S. H. Zhu<sup>77</sup> , T. J. Zhu<sup>12,g</sup> , W. D. Zhu<sup>12,g</sup> , W. J. Zhu<sup>1</sup> , W. Z. Zhu<sup>20</sup> ,  
Y. C. Zhu<sup>78,64</sup> , Z. A. Zhu<sup>1,70</sup> , X. Y. Zhuang<sup>47</sup> , J. H. Zou<sup>1</sup> 

(BESIII Collaboration)

<sup>1</sup> Institute of High Energy Physics, Beijing 100049, People's Republic of China

<sup>2</sup> Beihang University, Beijing 100191, People's Republic of China

<sup>3</sup> Bochum Ruhr-University, D-44780 Bochum, Germany

<sup>4</sup> Budker Institute of Nuclear Physics SB RAS (BINP), Novosibirsk 630090, Russia

<sup>5</sup> Carnegie Mellon University, Pittsburgh, Pennsylvania 15213, USA

<sup>6</sup> Central China Normal University, Wuhan 430079, People's Republic of China

<sup>7</sup> Central South University, Changsha 410083, People's Republic of China

<sup>8</sup> Chengdu University of Technology, Chengdu 610059, People's Republic of China

- <sup>25</sup> Huangshan College, Huangshan 245000, People's Republic of China
- <sup>26</sup> Hunan Normal University, Changsha 410081, People's Republic of China
- <sup>27</sup> Hunan University, Changsha 410082, People's Republic of China
- <sup>28</sup> Indian Institute of Technology Madras, Chennai 600036, India
- <sup>29</sup> Indiana University, Bloomington, Indiana 47405, USA
- <sup>30</sup> INFN Laboratori Nazionali di Frascati, (A)INFN Laboratori Nazionali di Frascati, I-00044, Frascati, Italy; (B)INFN Sezione di Perugia, I-06100, Perugia, Italy; (C)University of Perugia, I-06100, Perugia, Italy
- <sup>31</sup> INFN Sezione di Ferrara, (A)INFN Sezione di Ferrara, I-44122, Ferrara, Italy; (B)University of Ferrara, I-44122, Ferrara, Italy
- <sup>32</sup> Inner Mongolia University, Hohhot 010021, People's Republic of China
- <sup>33</sup> Institute of Business Administration, Karachi,
- <sup>34</sup> Institute of Modern Physics, Lanzhou 730000, People's Republic of China
- <sup>35</sup> Institute of Physics and Technology, Mongolian Academy of Sciences, Peace Avenue 54B, Ulaanbaatar 13330, Mongolia
- <sup>36</sup> Instituto de Alta Investigación, Universidad de Tarapacá, Casilla 7D, Arica 1000000, Chile
- <sup>37</sup> Jiangsu Ocean University, Lianyungang 222000, People's Republic of China
- <sup>38</sup> Jilin University, Changchun 130012, People's Republic of China
- <sup>39</sup> Johannes Gutenberg University of Mainz, Johann-Joachim-Becher-Weg 45, D-55099 Mainz, Germany
- <sup>40</sup> Joint Institute for Nuclear Research, 141980 Dubna, Moscow region, Russia
- <sup>41</sup> Justus-Liebig-Universität Giessen, II. Physikalisches Institut, Heinrich-Buff-Ring 16, D-35392 Giessen, Germany
- <sup>42</sup> Lanzhou University, Lanzhou 730000, People's Republic of China
- <sup>43</sup> Liaoning Normal University, Dalian 116029, People's Republic of China
- <sup>44</sup> Liaoning University, Shenyang 110036, People's Republic of China
- <sup>45</sup> Nanjing Normal University, Nanjing 210023, People's Republic of China
- <sup>46</sup> Nanjing University, Nanjing 210093, People's Republic of China
- <sup>47</sup> Nankai University, Tianjin 300071, People's Republic of China
- <sup>48</sup> National Centre for Nuclear Research, Warsaw 02-093, Poland
- <sup>49</sup> North China Electric Power University, Beijing 102206, People's Republic of China
- <sup>50</sup> Peking University, Beijing 100871, People's Republic of China
- <sup>51</sup> Qufu Normal University, Qufu 273165, People's Republic of China
- <sup>52</sup> Renmin University of China, Beijing 100872, People's Republic of China
- <sup>53</sup> Shandong Normal University, Jinan 250014, People's Republic of China
- <sup>54</sup> Shandong University, Jinan 250100, People's Republic of China
- <sup>55</sup> Shandong University of Technology, Zibo 255000, People's Republic of China
- <sup>56</sup> Shanghai Jiao Tong University, Shanghai 200240, People's Republic of China
- <sup>57</sup> Shanxi Normal University, Linfen 041004, People's Republic of China
- <sup>58</sup> Shanxi University, Taiyuan 030006, People's Republic of China
- <sup>59</sup> Sichuan University, Chengdu 610064, People's Republic of China
- <sup>60</sup> Soochow University, Suzhou 215006, People's Republic of China
- <sup>61</sup> South China Normal University, Guangzhou 510006, People's Republic of China
- <sup>62</sup> Southeast University, Nanjing 211100, People's Republic of China
- <sup>63</sup> Southwest University of Science and Technology, Mianyang 621010, People's Republic of China
- <sup>64</sup> State Key Laboratory of Particle Detection and Electronics, Beijing 100049, Hefei 230026, People's Republic of China
- <sup>65</sup> Sun Yat-Sen University, Guangzhou 510275, People's Republic of China
- <sup>66</sup> Suranaree University of Technology, University Avenue 111, Nakhon Ratchasima 30000, Thailand
- <sup>67</sup> Tsinghua University, Beijing 100084, People's Republic of China
- <sup>68</sup> Turkish Accelerator Center Particle Factory Group, (A)Istinye University, 34010, Istanbul, Turkey; (B)Near East University, Nicosia, North Cyprus, 99138, Mersin 10, Turkey
- <sup>69</sup> University of Bristol, H H Wills Physics Laboratory, Tyndall Avenue, Bristol, BS8 1TL, UK
- <sup>70</sup> University of Chinese Academy of Sciences, Beijing 100049, People's Republic of China
- <sup>71</sup> University of Groningen, NL-9747 AA Groningen, The Netherlands
- <sup>72</sup> University of Hawaii, Honolulu, Hawaii 96822, USA
- <sup>73</sup> University of Jinan, Jinan 250022, People's Republic of China
- <sup>74</sup> University of Manchester, Oxford Road, Manchester, M13 9PL, United Kingdom
- <sup>75</sup> University of Muenster, Wilhelm-Klemm-Strasse 9, 48149 Muenster, Germany
- <sup>76</sup> University of Oxford, Keble Road, Oxford OX13RH, United Kingdom
- <sup>77</sup> University of Science and Technology Liaoning, Anshan 114051, People's Republic of China
- <sup>78</sup> University of Science and Technology of China, Hefei 230026, People's Republic of China
- <sup>79</sup> University of South China, Hengyang 421001, People's Republic of China
- <sup>80</sup> University of the Punjab, Lahore-54590, Pakistan
- <sup>81</sup> University of Turin and INFN, (A)University of Turin, I-10125, Turin, Italy; (B)University of Eastern Piedmont, I-15121, Alessandria, Italy; (C)INFN, I-10125, Turin, Italy
- <sup>82</sup> Uppsala University, Box 516, SE-75120 Uppsala, Sweden
- <sup>83</sup> Wuhan University, Wuhan 430072, People's Republic of China
- <sup>84</sup> Yantai University, Yantai 264005, People's Republic of China

<sup>85</sup> Yunnan University, Kunming 650500, People's Republic of China

<sup>86</sup> Zhejiang University, Hangzhou 310027, People's Republic of China

<sup>87</sup> Zhengzhou University, Zhengzhou 450001, People's Republic of China

† Deceased

<sup>a</sup> Also at Bogazici University, 34342 Istanbul, Turkey

<sup>b</sup> Also at the Moscow Institute of Physics and Technology, Moscow 141700, Russia

<sup>c</sup> Also at the Novosibirsk State University, Novosibirsk, 630090, Russia

<sup>d</sup> Also at the NRC "Kurchatov Institute", PNPI, 188300, Gatchina, Russia

<sup>e</sup> Also at Goethe University Frankfurt, 60323 Frankfurt am Main, Germany

<sup>f</sup> Also at Key Laboratory for Particle Physics, Astrophysics and Cosmology, Ministry of Education; Shanghai Key Laboratory for Particle Physics and Cosmology; Institute of Nuclear and Particle Physics, Shanghai 200240, People's Republic of China

<sup>g</sup> Also at Key Laboratory of Nuclear Physics and Ion-beam Application (MOE) and Institute of Modern Physics, Fudan University, Shanghai 200443, People's Republic of China

<sup>h</sup> Also at State Key Laboratory of Nuclear Physics and Technology, Peking University, Beijing 100871, People's Republic of China

<sup>i</sup> Also at School of Physics and Electronics, Hunan University, Changsha 410082, China

<sup>j</sup> Also at Guangdong Provincial Key Laboratory of Nuclear Science, Institute of Quantum Matter, South China Normal University, Guangzhou 510006, China

<sup>k</sup> Also at MOE Frontiers Science Center for Rare Isotopes, Lanzhou University, Lanzhou 730000, People's Republic of China

<sup>l</sup> Also at Lanzhou Center for Theoretical Physics, Lanzhou University, Lanzhou 730000, People's Republic of China

<sup>m</sup> Also at Ecole Polytechnique Federale de Lausanne (EPFL), CH-1015 Lausanne, Switzerland

<sup>n</sup> Also at Helmholtz Institute Mainz, Staudinger Weg 18, D-55099 Mainz, Germany

<sup>o</sup> Also at Hangzhou Institute for Advanced Study, University of Chinese Academy of Sciences, Hangzhou 310024, China

<sup>p</sup> Currently at Silesian University in Katowice, Chorzow, 41-500, Poland

<sup>q</sup> Also at Applied Nuclear Technology in Geosciences Key Laboratory of Sichuan Province, Chengdu University of Technology, Chengdu 610059, People's Republic of China

(Dated: **March 10, 2026**)

Using a sample of  $e^+e^-$  annihilation data corresponding to an integrated luminosity of  $4.4 \text{ fb}^{-1}$  collected with the BESIII detector at the BEPCII collider and produced at center-of-mass energies from 4600 to 4698 MeV, an amplitude analysis is performed of the singly Cabibbo-suppressed decay  $\Lambda_c^+ \rightarrow pK^+K^-$ . The branching fractions of  $\Lambda_c^+ \rightarrow p\phi(1020)$ ,  $pf_0(980)$ ,  $\Lambda(1405)K^+$ , and  $\Lambda(1670)K^+$  are measured, where the latter two modes are decays that are observed for the first time. At the same time, with the detection efficiency based on the results of the amplitude analysis, the branching fraction of  $\Lambda_c^+ \rightarrow pK^+K^-$  is updated to be  $(9.94 \pm 0.65_{\text{stat.}} \pm 0.50_{\text{syst.}}) \times 10^{-4}$ , which is consistent with the current world average value within one standard deviation. The result supersedes the previous BESIII measurement with precision improved by approximately a factor of 1.5.

## I. INTRODUCTION

Charmed baryons were first observed in the 1970s, with the lightest one,  $\Lambda_c^+$ , sparking extensive research into the properties and structure of the charmed baryon family [1]. Distinct from the subsequently discovered  $\Xi_c^{+,0}$  and  $\Omega_c^0$  baryons, the  $\Lambda_c^+$  provides a comparatively simple system for exploring the dynamics of charmed baryons [2]. It also offers crucial insights into the structure and decay mechanisms of doubly charmed baryons such as  $\Xi_{cc}$  and  $\Omega_{cc}$  [3].

Quantum chromodynamics (QCD) [4, 5], the fundamental theory describing the strong interaction among quarks and gluons, plays a central role in predicting the decay of quarks bound within charmed baryons. Among the various decay categories, singly Cabibbo-suppressed (SCS) decays are of particular interest because of their sensitivity to charge-parity ( $CP$ ) violation. These decays can carry a significant weak phase, thereby providing enhanced sensitivity to possible  $CP$ -violating effects beyond the Standard Model [6, 7].

The SCS decay  $\Lambda_c^+ \rightarrow pK^+K^-$  is regarded as a golden channel for investigating  $CP$  violation in charmed baryon decays, owing to its relatively large branching fraction and favorable detection efficiency. A comprehensive study of the intermediate resonant contributions in this decay is vital for improving our understanding of the underlying decay dynamics and for refining searches for  $CP$  violation. Moreover, the use of high-precision signal models allows for a more accurate description of signal behavior in experimental data, which is essential for reliably identifying and quantifying possible  $CP$ -violating effects in baryonic systems.

Situated at the interface between perturbative and non-perturbative QCD regimes, the charm quark's role in this decay has attracted considerable theoretical attention, particularly in the  $\Lambda_c^+ \rightarrow p\phi(1020)$  channel, which dominates the  $\Lambda_c^+ \rightarrow pK^+K^-$  decay. The corresponding Feynman diagrams for  $\Lambda_c^+ \rightarrow pK^+K^-$  and  $\Lambda_c^+ \rightarrow p\phi(1020)$  are shown in Fig. 1. The  $\Lambda_c^+ \rightarrow p\phi(1020)$  process is comparatively simple, proceeding primarily through the factorizable diagram (Fig. 1(c)) [8]. However, theoretical predictions for this channel differ

significantly among models [9–14], as summarized— together with available experimental measurements—in Table I.

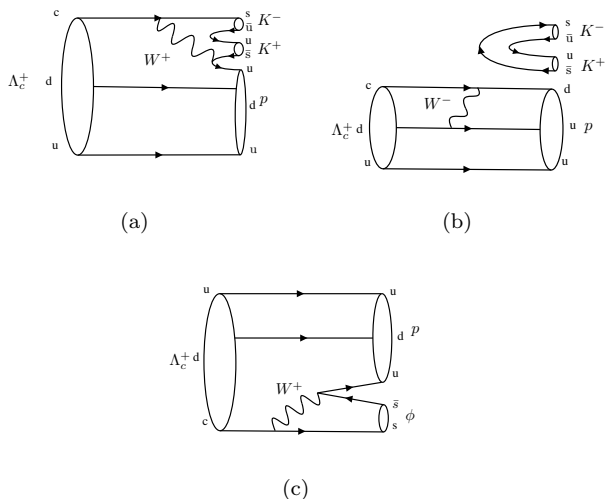


FIG. 1. Feynman diagrams of  $\Lambda_c^+ \rightarrow pK^+K^-$  via internal W-emission (a),  $\Lambda_c^+ \rightarrow pK^+K^-$  via W-exchange (b), and  $\Lambda_c^+ \rightarrow p\phi(1020)$  via internal W-emission (c).

Using  $4.4 \text{ fb}^{-1}$  of  $e^+e^-$  annihilation data collected at the center-of-mass (CM) energies 4600, 4628, 4641, 4661, 4682, and 4698 MeV with the BESIII detector at the BEPCII collider [15], we perform the first amplitude analysis of the decay  $\Lambda_c^+ \rightarrow pK^+K^-$  and determine its branching fraction with improved precision.

The amplitude analysis provides a powerful tool for disentangling the contributing intermediate states and their interferences, offering more profound insight into the decay dynamics of charmed baryons. In particular, it allows the identification of structures in the  $pK^-$  invariant mass spectrum, thereby refining the modeling of signal components and reducing systematic uncertainties in the branching fraction measurement.

## II. BESIII DETECTOR AND MONTE CARLO SIMULATION

The BESIII detector [16] records symmetric  $e^+e^-$  collisions provided by the BEPCII storage ring [17] in the CM energy ranging from 1.84 to 4.95 GeV, with a peak luminosity of  $1.1 \times 10^{33} \text{ cm}^{-2}\text{s}^{-1}$  achieved at  $\sqrt{s} = 3.773 \text{ GeV}$ . BESIII has collected large data samples in this energy region [18]. The cylindrical core of the BESIII detector covers 93% of the full solid angle and consists of a helium-based multilayer drift chamber (MDC), a plastic scintillator time-of-flight system (TOF), and a CsI(Tl) electromagnetic calorimeter (EMC), which are all enclosed in a superconducting solenoidal magnet providing a 1.0 T magnetic field. The solenoid is supported by an octagonal flux-return yoke with resistive

plate counter muon identification modules interleaved with steel. The charged-particle momentum resolution at 1 GeV/c is 0.5%, and the specific ionization energy loss in the MDC ( $dE/dx$ ) resolution is 6% for electrons from Bhabha scattering. The EMC measures photon energies with a resolution of 2.5% (5%) at 1 GeV in the barrel (end cap) region. The time resolution in the plastic scintillator TOF barrel region is 68 ps, while that in the end cap region is 110 ps. The end cap TOF system was upgraded in 2015 using multigap resistive plate chamber technology, providing a time resolution of 60 ps [19].

Monte Carlo (MC) simulated data samples produced with a GEANT4-based [20] software package, which includes the geometric description of the BESIII detector and the detector response, which are used to determine detection efficiencies and to estimate backgrounds. The simulation models the beam energy spread and initial state radiation (ISR) in the  $e^+e^-$  annihilations with the generator KKMC [21]. The inclusive MC sample includes the production of open charm processes, the initial state radiation production of vector charmonium(-like) states, and the continuum processes incorporated in KKMC [21]. All particle decays are modeled with EVTGEN [22] using branching fractions either taken from the Particle Data Group (PDG) [23], where available, or otherwise estimated with LUNDCHARM [24]. Final state radiation from charged final state particles is incorporated using the PHOTOS package [25]. The signal MC samples for amplitude analysis and branching fraction measurement are generated using different models. For the amplitude analysis, a phase space (PHSP) MC sample is used in the MC integration. While for the branching fraction measurement, the signal MC sample is generated based on the result of amplitude analysis for a more accurate efficiency.

## III. EVENT SELECTION

Charged tracks detected in the MDC are required to satisfy  $|\cos\theta| < 0.93$ , where  $\theta$  is the polar angle with respect to the  $z$ -axis, defined as the symmetry axis of the MDC. Each track must have a distance of closest approach to the interaction point (IP) of less than 10 cm along the beam direction ( $V_z$ ) and less than 1 cm in the transverse plane ( $V_r$ ). Particle identification (PID) for charged tracks combines measurements of the ionization energy loss ( $dE/dx$ ) in the MDC and the flight time measured by the TOF system. For each charged particle hypothesis  $h = (p, K, \pi)$ , a corresponding likelihood  $\mathcal{L}(h)$  is calculated. A track is identified as a proton if  $\mathcal{L}(p) > \mathcal{L}(K)$  and  $\mathcal{L}(p) > \mathcal{L}(\pi)$ . Similarly, charged kaons and pions are identified according to the larger likelihood between the kaon and pion hypotheses, i.e.,  $\mathcal{L}(K) > \mathcal{L}(\pi)$  or  $\mathcal{L}(\pi) > \mathcal{L}(K)$ , respectively.

An additional requirement of  $V_r < 0.2 \text{ cm}$  is imposed on proton candidates to suppress background protons originating from beam-related interactions or secondary

TABLE I. Predictions for and measurements of branching fractions for  $\Lambda_c^+ \rightarrow pK^+K^-$  and  $\Lambda_c^+ \rightarrow p\phi(1020)$ . The superscript “\*” indicates a range of predicted values that depend on the renormalization scheme used in the corresponding theoretical model.

Prediction or measurement	$\Lambda_c^+ \rightarrow pK^+K^-$ (%)	$\Lambda_c^+ \rightarrow p\phi(1020)$ (%)
Körner(1992), CCQM [9]	...	0.003
Żencaykowski(1994), Pole [10]	...	0.10
Żencaykowski(1994), Pole [11]	...	0.14
Alakabha Datta(1995), CA [12]	...	0.063
Cheng, Tseng(1993), Pole [13]	...	0.073
Ivanov(1998), CCQM [14]	...	0.138 – 0.657*
CLEO(1996) [26]	$0.244 \pm 0.056 \pm 0.044$	$0.150 \pm 0.038 \pm 0.019$
Belle(2002) [27]	$0.088 \pm 0.013 \pm 0.013$	$0.094 \pm 0.013 \pm 0.013$
BESIII(2016) [28]	$0.107 \pm 0.016 \pm 0.007$	$0.106 \pm 0.019 \pm 0.010$
LHCb(2018) [29]	$0.106 \pm 0.002 \pm 0.005$	...
PDG(2024) [23]	$0.106 \pm 0.006$	$0.106 \pm 0.014$

processes. Such backgrounds may arise from interactions of the electron/positron beams or final-state particles with the inner wall of the MDC or residual gas inside the beam pipe, as discussed in Ref. [28].

With the preliminarily selected proton and kaon candidates,  $\Lambda_c^+$  signal candidates are reconstructed from all possible combinations of  $pK^+K^-$ . Two kinematic variables related to energy and momentum conservation are used to identify  $\Lambda_c^+$  candidates. The first variable is the energy difference, defined as  $\Delta E = E - E_{\text{beam}}$ , where  $E$  is the total reconstructed energy of the  $\Lambda_c^+$  candidate in the  $e^+e^-$  CM system and  $E_{\text{beam}}$  is the calibrated beam energy. The  $\Lambda_c^+$  signal is expected to peak near zero in the  $\Delta E$  distribution. The second variable is the beam-energy-constrained mass,  $M_{\text{BC}} \equiv \sqrt{E_{\text{beam}}^2/c^4 - |\vec{p}|^2/c^2}$ , where  $\vec{p}$  is the reconstructed total momentum of the  $\Lambda_c^+$  candidate in the CM frame. To obtain a clean sample of  $\Lambda_c^+$  candidates, loose preselection requirements are applied:  $|\Delta E| < 0.1$  GeV and  $M_{\text{BC}} > 2.25$  GeV/ $c^2$ . If multiple candidates satisfy these conditions within a single event, the candidate with the smallest  $|\Delta E|$  is retained. The selection of the optimal  $\Delta E$  window is further refined by maximizing the Figure of Merit (FOM), defined as  $\text{FOM} = \frac{S}{\sqrt{S+B}} \times \frac{S}{S+B}$  [30, 31], where  $S$  and  $B$  denote the numbers of signal and background events, respectively, estimated from inclusive background MC samples. For the amplitude analysis, a stringent requirement of  $|\Delta E| < 0.005$  GeV is imposed, while for the branching fraction measurement, a looser selection of  $|\Delta E| < 0.02$  GeV is applied. To evaluate the residual combinatorial background that survives the selection criteria, an unbinned maximum-likelihood fit to the  $M_{\text{BC}}$  distribution is performed separately for each energy point. In the fit, the signal is modeled using an MC-simulated shape convolved with a Gaussian function to account for small discrepancies between data and simulation due to imperfect detector modeling and

beam-energy spread. The background is described by an ARGUS function [32], defined as

$$f(M_{\text{BC}}, E_0, c, p) = M_{\text{BC}} \left( 1 - \left( \frac{M_{\text{BC}}}{E_0} \right)^2 \right)^p \times e^{c \cdot \left( 1 - \frac{M_{\text{BC}}}{E_0} \right)^2},$$

where  $E_0$  is the endpoint of  $M_{\text{BC}}$  fixed to the beam energy,  $p$  is the power parameter (fixed to 0.5 by default), and  $c$  is a free scale factor. The total probability density function (PDF) is expressed as the sum of the signal and the background components.

Based on the fits to the  $M_{\text{BC}}$  distributions of data at each individual energy point, the background-shape parameters obtained from the corresponding fit are fixed in the subsequent analyses that employ the *sPlot* technique [33]. This method assigns event-by-event statistical weights, known as sWeights, which are derived as a function of a discriminating variable (here,  $M_{\text{BC}}$ ). These weights are constructed such that the signal distribution is statistically normalized, while being orthogonal to the background distribution. Consequently, after applying the sWeights, background contributions are effectively removed from the signal distribution. The resulting weighted sample is used for the amplitude analysis to ensure a high-purity signal dataset. By combining data from all energy points, a total of  $353 \pm 22$  signal events is obtained.

#### IV. AMPLITUDE ANALYSIS

Once all selection criteria have been applied, the remaining signal events are used for the amplitude analysis. This analysis is performed using the helicity amplitude formalism [34, 35], implemented within the open-source framework TF-PWA [36].

For a generic two-body decay process of the form  $1 \rightarrow$

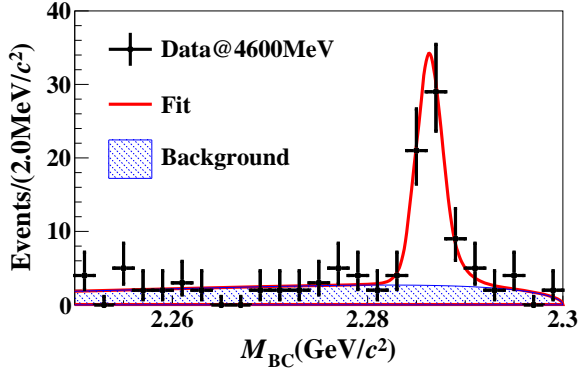


FIG. 2. Fit to the  $M_{BC}$  distribution of the accepted candidates for  $\Lambda_c^+ \rightarrow pK^+K^-$  at 4600 MeV. The black dots with error bars represent the data, and the blue-shaded region indicates the combinatorial background.  $|\Delta E| < 0.02$  GeV is applied in this figure.

$2 + 3$ , the helicity amplitude can be expressed as

$$A_{\lambda_1, \lambda_2, \lambda_3}^{1 \rightarrow 2+3} = H_{\lambda_2, \lambda_3}^{1 \rightarrow 2+3} D_{\lambda_1, \lambda_2 - \lambda_3}^{J_1}(\phi, \theta, 0),$$

where  $J$  and  $\lambda$  denote the spin and helicity of the respective particles. The amplitude  $H_{\lambda_2, \lambda_3}^{1 \rightarrow 2+3}$  is parameterized using the LS coupling formalism [37], which includes the Blatt–Weisskopf barrier factor [38]. In this framework, the LS coupling strengths serve as the direct fit parameters of the analysis.

As an illustrative example, consider the decay chain  $e^+e^- \rightarrow \Lambda_c^+ \bar{\Lambda}_c^-$ , followed by  $\Lambda_c^+ \rightarrow \Lambda^* K^+$ . The corresponding helicity angles and cascade decay topology are depicted in Fig. 3. In the Wigner  $D$ -function  $D_{\lambda_1, \lambda_2 - \lambda_3}^{J_1}(\phi, \theta, 0)$ , the variables  $\phi$  and  $\theta$  denote the helicity angles defined as shown in Fig. 3.

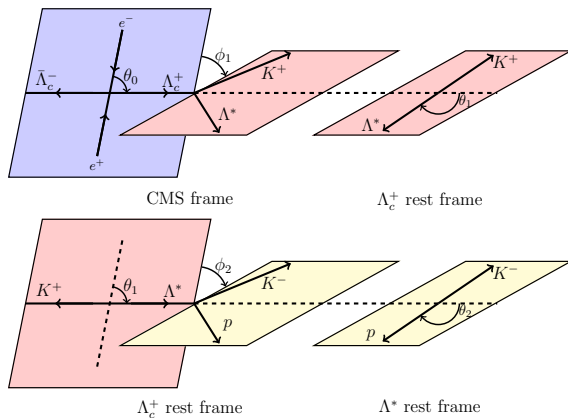


FIG. 3. Definition of the helicity frame for  $e^+e^- \rightarrow \Lambda_c^+ \bar{\Lambda}_c^-$ ,  $\Lambda_c^+ \rightarrow \Lambda^* K^+$ .

The amplitudes are constructed from  $e^+e^-$  to the final two-body decays. The parameters describing the amplitude from  $\Lambda_c^+$  decays to the final two-body state are shared for all energy points.

The full amplitude for each component is the product of every two body decay amplitude and the corresponding dynamic part. For example, in the  $\Lambda_c^+ \rightarrow pK^+K^-$  decay, the amplitude of the  $pK^-$  ( $\Lambda^*$ ) resonance is defined as

$$A_{\lambda_{\gamma^*}, \lambda_p}^{\Lambda^*} = \sum_{\lambda_{\bar{\Lambda}_c^-}} A_{\lambda_{\gamma^*}, \lambda_{\Lambda_c^+}, \lambda_{\bar{\Lambda}_c^-}}^{\gamma^* \rightarrow \Lambda_c^+ \bar{\Lambda}_c^-} A_{\lambda_{\Lambda_c^+}, \lambda_{\Lambda^*}, 0}^{\Lambda_c^+ \rightarrow \Lambda^* K^+} R_{\Lambda^*}(M_{pK^-}) A_{\lambda_{\Lambda^*}, \lambda_p, 0}^{\Lambda^* \rightarrow pK^-}.$$

To enhance the precision of the  $\Lambda_c^+$  decay amplitude measurement, the decay parameters of  $e^+e^- \rightarrow \Lambda_c^+ \bar{\Lambda}_c^-$  are fixed according to the BESIII measurement [39]. For the  $\Lambda_c^+$  decay, the three-body decay is described by several quasi-two-body sequential two-step decays. The amplitude for a full decay chain contains a propagator  $R$  [40], using different models for different resonances. For the  $\Lambda(1670)$  and  $\phi(1020)$  resonances, their line shapes are described with the relativistic Breit-Wigner formula [40]

$$R(m) = \frac{1}{m_0^2 - m^2 - im_0\Gamma(m)},$$

where  $\Gamma(m)$  is the mass-dependent width. The nominal mass and width of  $\Lambda(1670)$  are taken from the PDG [23] while they are free parameters for  $\phi(1020)$ . For  $\Lambda(1405)$  and  $f_0(980)$ , their line shapes are described with a two-coupled-channels Flatté model [41]

$$R(m) = \frac{1}{m_0^2 - m^2 - i(g_1\rho_1 + g_2\rho_2)}$$

with phase-space factors  $\rho_k$  and coupling strengths  $g_k$ . For  $f_0(980)$ , channels 1 and 2 denote the coupled channels  $\pi\pi$  and  $KK$  [42], while they denote  $pK$  and  $\Sigma\pi$  for  $\Lambda(1405)$  [43].

Finally, the total amplitude is derived by summing the amplitudes of all possible resonances as

$$\begin{aligned} \mathcal{A}_{\lambda_{\gamma^*}, \lambda_p}^{\text{total}} &= A_{\lambda_{\gamma^*}, \lambda_p}^{\phi} + A_{\lambda_{\gamma^*}, \lambda_p}^{f_0/a_0(980)} \\ &+ \sum_{\lambda'_p} \left( \sum A_{\lambda_{\gamma^*}, \lambda_p}^{\Lambda^*} \right) D_{\lambda'_p, \lambda_p}^{1/2}(\alpha_p, \beta_p, \gamma_p) \end{aligned}$$

where the extra  $D$ -function is added to align the spins of the final-state protons from different decay chains.

The construction of the signal PDF and the derivation of the fit fraction (FF), interference, and the corresponding statistical uncertainties follow the methodologies employed in the previous BESIII measurement [40]. Taking  $\Lambda(1670)$  as an example, the FF is defined to be

$$\text{FF} = \frac{\mathcal{B}(\Lambda_c^+ \rightarrow \Lambda(1670)K^+, \Lambda(1670) \rightarrow pK^-)}{\mathcal{B}(\Lambda_c^+ \rightarrow pK^+K^-)}.$$

The negative log likelihood (NLL) is calculated as the sum over all signal candidates, weighted by the sWeight

factor  $w_i$  [33],

$$-\ln L = -a \sum_{i \in \text{data}} w_i \ln P(p_i),$$

with the normalization factor  $a = \frac{\sum_{i \in \text{data}} w_i}{\sum_{i \in \text{data}} w_i^2}$  [44].

To establish the baseline solution for the amplitude analysis, a statistical significance test is performed for each possible intermediate component. Distinct structures corresponding to  $\phi(1020)$ ,  $\Lambda(1405)$ , and  $\Lambda(1670)$  are clearly observed in the  $K^+K^-$  and  $pK^-$  invariant mass spectra; hence, these components are incorporated into the baseline model. The statistical significance of each component is evaluated by comparing the change in the negative log-likelihood (NLL) between fits with and without the component, while accounting for the associated change in the number of degrees of freedom. As a result, the baseline solution includes the  $\phi(1020)$ ,  $f_0(980)$ ,  $\Lambda(1405)$ , and  $\Lambda(1670)$  resonant components, with no evidence for a significant nonresonant contribution. For the  $\phi(1020)$  resonance, its intrinsic width is comparable to the detector resolution; therefore, resolution effects must be taken into account. These effects are incorporated into the probability density function (PDF) by convolving the line shape with a detector resolution function. The resolution parameters are obtained by fitting the  $K^+K^-$  invariant mass spectrum with a Breit-Wigner line shape convolved with a double-Gaussian resolution model. To accurately describe the resolution effects in the  $\Lambda_c^+ \rightarrow pK^+K^-$  decay, the relationship between the true and reconstructed momenta is integrated into the model. The resulting PDF is expressed as a weighted sum of amplitude squares, modulated by detector effects, providing a precise description of the decay dynamics and an effective treatment of the experimental resolution.

The projections of the fit results on the invariant mass spectra are shown in Fig. 4, and the obtained fit fractions (FFs) together with their statistical significances are summarized in Table II. To validate the stability and reliability of the fit procedure, an input-output (IO) test is performed using 500 pseudoexperiments (“toy” samples), each containing the same number of events as the data. Each toy sample includes both signal and background contributions: the signal is generated using the central values from the nominal fit, while the background is modeled using inclusive and hadronic MC samples. The effects of the detector efficiency are appropriately incorporated into each simulated sample. The fitted FFs and their statistical uncertainties from the nominal fit are then corrected based on the pull distributions obtained from the IO test.

## V. BRANCHING FRACTION MEASUREMENT

Using the amplitude model obtained from the analysis, a more precise measurement of the branching fraction

TABLE II. The FFs and statistical significances ( $\mathcal{S}$ ) for different components in the baseline solution. The total FF is 130%. The first uncertainty is statistical, and the second is systematic.

Process	FF (%)	$\mathcal{S}$
$p\phi(1020)$	$57 \pm 5 \pm 2$	$16.6\sigma$
$pf_0(980)$	$40 \pm 16 \pm 15$	$3.6\sigma$
$\Lambda(1405)K^+$	$21 \pm 9 \pm 6$	$4.6\sigma$
$\Lambda(1670)K^+$	$12 \pm 10 \pm 8$	$5.0\sigma$

of  $\Lambda_c^+ \rightarrow pK^+K^-$  is performed. As mentioned earlier, a relaxed requirement of  $|\Delta E| < 0.02$  GeV is applied in this part of the study. In the nominal fit, a simultaneous fit to the  $M_{BC}$  distributions at six center-of-mass energies is carried out, with a common branching fraction shared among all energy points. The signal component is described by the signal MC shape derived from the amplitude analysis, convolved with a Gaussian resolution function whose parameters are left free in the fit. At each energy point, 100,000 signal MC events are generated to model the signal shape. The Gaussian parameters are constrained to be the same across all energy points to ensure a consistent description of the resolution. The background is modeled with an ARGUS function [32], where the endpoint parameter is fixed to the beam energy  $E_{\text{beam}}$  corresponding to each energy point. The detection efficiency is determined from signal MC samples. For each energy point, a dedicated sample of 1,000,000 simulated events is generated, in which one of the  $\Lambda_c^+(\bar{\Lambda}_c^-)$  baryons decays into the signal mode and the other into all possible final states. The detection efficiency is obtained by counting the number of reconstructed signal events that satisfy all selection criteria within the signal region. The efficiencies determined for the six energy points are summarized in Table III.

TABLE III. Detection efficiencies for each decay mode at six energy points.

$\sqrt{s}$ (MeV)	$\epsilon_i$ (%)	$N_{\text{sig}}^i$
4600	$39.55 \pm 0.05$	$76.9 \pm 5.0$
4628	$36.62 \pm 0.05$	$65.2 \pm 4.3$
4641	$36.11 \pm 0.05$	$68.9 \pm 4.5$
4661	$35.10 \pm 0.05$	$65.9 \pm 4.3$
4682	$34.08 \pm 0.05$	$193.0 \pm 12.6$
4698	$33.33 \pm 0.05$	$55.7 \pm 3.6$

The branching fraction is determined by

$$\mathcal{B} = \frac{N_{\text{sig}}^i}{2 \cdot [N_{(\Lambda_c^+ \bar{\Lambda}_c^-)_i} \cdot \epsilon_i]}, (i = 1, 6),$$

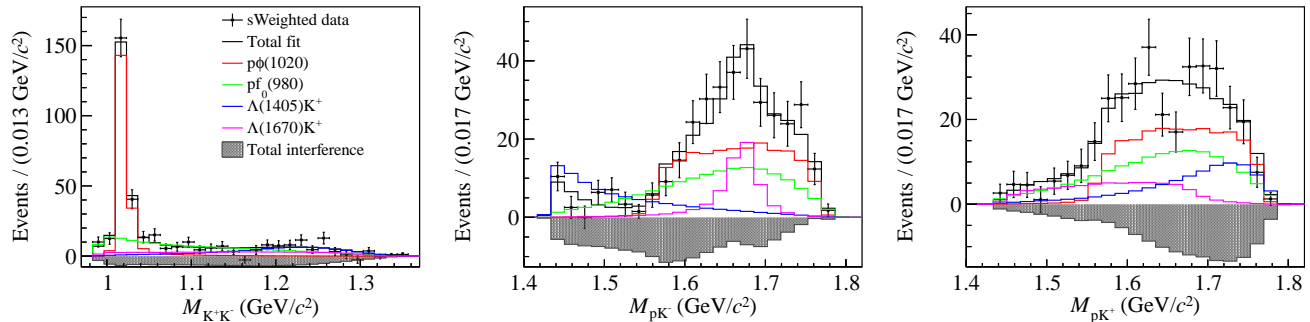


FIG. 4. Projections of the amplitude fit results on the  $M_{K^+K^-}$ ,  $M_{pK^-}$ , and  $M_{pK^+}$  spectra. The points with error bars are weighted data at all energy points. Different colored curves represent different components, as shown in the legend.

where  $N_{(\Lambda_c^+\bar{\Lambda}_c^-)_i}$  is number of the  $\Lambda_c^+\bar{\Lambda}_c^-$  pairs at the  $i$ -th energy point, taken from Ref. [45]. The branching fraction for  $\Lambda_c^+ \rightarrow pK^+K^-$  is a fit parameter. Finally, the fit returns a signal yield of  $526 \pm 34$  events, and the branching fraction of  $\Lambda_c^+ \rightarrow pK^+K^-$  is measured to be  $(9.94 \pm 0.65) \times 10^{-4}$ .

## VI. SYSTEMATIC UNCERTAINTIES

In the amplitude analysis, systematic uncertainties arise from several sources, including resonance parameters, the radius parameter, background size, background shape, resonant components, polarization parameters, and the discrepancy between data and MC simulations.

The systematic uncertainties associated with the resonance parameters originate from the fixed values used to describe each resonance. To estimate these uncertainties, Gaussian sampling is performed using the central values and standard deviations of the fixed parameters. For each sampled set, the amplitude fit is repeated, and the resulting distribution of each FF is fitted with a Gaussian function; the corresponding standard deviation is taken as the systematic uncertainty. Systematic uncertainties related to the Blatt–Weisskopf barrier radius parameter are evaluated by varying  $p_r = 1/d$  within the range 0.17 GeV/c to 0.37 GeV/c, as recommended in Ref. [46]. The uncertainty due to the background yield is estimated by varying the background normalization by  $\pm 1\sigma$  in the  $sPlot$  procedure and repeating the sWeight extraction for the amplitude analysis. For the background shape, the systematic effect is assessed by replacing the nominal ARGUS function with the background shape derived from MC simulation in the  $sPlot$  procedure, followed by a re-extraction of the sWeights and repetition of the amplitude fit. The possible influence of additional resonant components is investigated by including an extra, statistically insignificant resonance— $\Lambda(1520)$ —in the fit. The resulting variation in the fit results is assigned as a systematic uncertainty. To account for the uncertainty associated with the polarization parameter, 500 pseudoexperiments are generated by

Gaussian sampling of the fixed polarization values. The amplitude fit is repeated for each sample, and the standard deviation of the 500 results is taken as the corresponding systematic uncertainty. Finally, the systematic uncertainty arising from differences between data and MC simulation is evaluated using correction factors that quantify efficiency discrepancies. These factors are defined as  $\omega = \varepsilon_{\text{data}}/\varepsilon_{\text{MC}}$ , where  $\varepsilon_{\text{data}}$  and  $\varepsilon_{\text{MC}}$  are the detection efficiencies obtained from control samples in data and MC simulation, respectively. The correction factors are applied to reweight the PHSP MC samples, and the full fit procedure is repeated to estimate the resulting systematic variation. The resulting systematic uncertainties of the amplitude analysis are listed in Table IV.

The systematic uncertainties in the branching fraction measurement arise from the following sources: tracking efficiency, particle identification (PID), the total number of produced  $\Lambda_c^+\bar{\Lambda}_c^-$  pairs ( $N_{\Lambda_c^+\bar{\Lambda}_c^-}$ ), the  $M_{\text{BC}}$  fit, the  $\Delta E$  selection requirement, and the MC signal model. The uncertainties associated with the tracking and PID efficiencies of charged particles are estimated to be 1% per track. These values are determined using control samples from the processes  $e^+e^- \rightarrow \pi^+\pi^+\pi^-\pi^-$  and  $e^+e^- \rightarrow K^+K^-\pi^+\pi^-$  collected at CM energies above  $\sqrt{s} = 4.0$  GeV [47]. The uncertainty arising from the  $M_{\text{BC}}$  fit is evaluated to be 1.3% by comparing results obtained when fixing the background-shape parameters to those determined from background MC samples. The uncertainty due to the  $\Delta E$  selection requirement is estimated by varying the resolution of the  $\Delta E$  distribution, resulting in an uncertainty of 0.2%. For the MC signal model, the signal shape is derived from simulated samples generated using the amplitude model obtained in the nominal fit. To assess the model-related uncertainty, the amplitude parameters are randomly varied according to their nominal values and uncertainties in 100 iterations. For each iteration, the full fit procedure is repeated to re-evaluate the efficiency and branching fraction. The resulting branching fraction distribution is fitted with a Gaussian function, and the ratio of its standard deviation to the nominal branching fraction value (1.6%) is assigned as the systematic

TABLE IV. The systematic uncertainties of the amplitude analysis.

Source	FF $_{\phi(1020)}$ (%)	FF $_{f_0(980)}$ (%)	FF $_{\Lambda(1405)}$ (%)	FF $_{\Lambda(1670)}$ (%)
Resonance parameter	0.8	34.8	23.0	39.8
Radius parameter	2.1	1.8	4.3	2.4
Background size	0.5	10.2	4.7	6.8
Background shape	0.7	1.7	7.5	13.3
Resonant component	1.0	16.4	19.2	13.3
Polarization parameter	0.3	3.2	2.6	7.0
Data/MC difference	0.6	1.2	1.9	0.6
Total	2.7	40.0	31.7	45.1

TABLE V. The relative systematic uncertainties in the branching fraction measurement.

Source	$\Lambda_c^+ \rightarrow pK^+K^-$ (%)
Tracking	3.0
PID	3.0
$\Delta E$ requirement	0.2
Background shape	1.3
MC model	1.6
$N_{\Lambda_c^+ \bar{\Lambda}_c^-}$	1.7
Total	5.0

uncertainty. Finally, the uncertainty in the total number of  $\Lambda_c^+ \bar{\Lambda}_c^-$  pairs,  $N_{\Lambda_c^+ \bar{\Lambda}_c^-}$ , is taken to be 1.7%, as quoted from Ref. [45]. The resulting systematic uncertainties in the branching fraction measurement are listed in Table V.

## VII. SUMMARY

To summarize, based on  $e^+e^-$  collision data corresponding to an integrated luminosity of  $4.4 \text{ fb}^{-1}$

$$\begin{aligned}
\mathcal{B}(\Lambda_c^+ \rightarrow \Lambda(1405)K^+, \Lambda(1405) \rightarrow pK^-) &= (0.23 \pm 0.10 \pm 0.06 \pm 0.01) \times 10^{-3}, \\
\mathcal{B}(\Lambda_c^+ \rightarrow \Lambda(1670)K^+, \Lambda(1670) \rightarrow pK^-) &= (0.13 \pm 0.11 \pm 0.09 \pm 0.01) \times 10^{-3}, \\
\mathcal{B}(\Lambda_c^+ \rightarrow pf_0(980), f_0(980) \rightarrow K^+K^-) &= (0.43 \pm 0.17 \pm 0.16 \pm 0.02) \times 10^{-3}, \\
\mathcal{B}(\Lambda_c^+ \rightarrow p\phi(1020), \phi(1020) \rightarrow K^+K^-) &= (0.62 \pm 0.05 \pm 0.02 \pm 0.03) \times 10^{-3}.
\end{aligned} \tag{1}$$

The branching fraction of  $\Lambda_c^+ \rightarrow p\phi(1020)$  is measured to be  $(1.21 \pm 0.11 \pm 0.08 \pm 0.01) \times 10^{-3}$ , representing the most precise determination to date. This value agrees well with theoretical predictions from the pole model [10, 11] and the covariant confined quark model (CCQM) [14], and is consistent with previous experimental results and the PDG average.

collected with the BESIII detector at CM energies between 4600 and 4698 MeV, an amplitude analysis of the charmed baryon decay  $\Lambda_c^+ \rightarrow pK^+K^-$  has been performed. Using the amplitude model derived from this analysis, the relative branching fractions of the resonant components are measured for the first time. By combining these results with the most precise value of  $\mathcal{B}(\Lambda_c^+ \rightarrow pK^+K^-) = (1.08 \pm 0.05) \times 10^{-3}$  reported by the PDG [23], the absolute branching fractions of the individual resonant components are obtained, as summarized in Eq. 1. The quoted uncertainties are, in order, statistical, systematic, and from the PDG reference value. Since the PDG provides averages with higher precision than our own result, it is adopted to reduce the overall uncertainty.

From the amplitude analysis, the overall branching fraction of  $\Lambda_c^+ \rightarrow pK^+K^-$  is determined to be  $(9.94 \pm 0.65 \pm 0.50) \times 10^{-4}$ . This result improves upon the precision of the previous BESIII measurement [28] by approximately a factor of 1.5. Our measurement is consistent with other experimental results, but deviates from the CLEO measurement,  $(2.44 \pm 0.56 \pm 0.44) \times$

$10^{-3}$  [26], by about  $2.0\sigma$ . These results provide valuable input for understanding the dynamics of charmed baryon decays and contribute to the broader study of hadronic decay mechanisms and possible  $CP$ -violating effects in the charm sector.

The BESIII Collaboration thanks the staff of BEPCII (<https://cstr.cn/31109.02.BEPC>) and the IHEP computing center for their strong support. This work is supported in part by National Key R&D Program of China under Contracts Nos. 2023YFA1606000, 2023YFA1606704, 2023YFA1609400; National Natural Science Foundation of China (NSFC) under Contracts Nos. 11635009, 11935015, 11935016, 11935018, 12025502, 12035009, 12035013, 12061131003, 12105127, 12192260, 12192261, 12192262, 12192263, 12192264, 12192265, 12221005, 12225509, 12235017, 12361141819, 12422504; the Chinese Academy of Sciences (CAS) Large-Scale Scientific Facility Program; the Strategic Priority Research Program of Chinese Academy of

Sciences under Contract No. XDA0480600; CAS under Contract No. YSBR-101; 100 Talents Program of CAS; Fundamental Research Funds for the Central Universities, Lanzhou University under Contracts Nos. lzujbky-2023-stlt01, lzujbky-2025-ytB01; The Institute of Nuclear and Particle Physics (INPAC) and Shanghai Key Laboratory for Particle Physics and Cosmology; ERC under Contract No. 758462; German Research Foundation DFG under Contract No. FOR5327; Istituto Nazionale di Fisica Nucleare, Italy; Knut and Alice Wallenberg Foundation under Contracts Nos. 2021.0174, 2021.0299; Ministry of Development of Turkey under Contract No. DPT2006K-120470; National Research Foundation of Korea under Contract No. NRF-2022R1A2C1092335; National Science and Technology fund of Mongolia; Polish National Science Centre under Contract No. 2024/53/B/ST2/00975; STFC (United Kingdom); Swedish Research Council under Contract No. 2019.04595; U. S. Department of Energy under Contract No. DE-FG02-05ER41374.

- 
- [1] G. S. Abrams, M. S. Alam, C. A. Blocker, A. Boyarski, M. Breidenbach, D. L. Burke, W. C. Carithers, W. Chinowsky, M. W. Coles and S. Cooper, *et al. Phys. Rev. Lett.* **44**, 10 (1980).
- [2] P. R. Li, X. R. Lyu and Y. Zheng, *Chin. Phys.* **50**, no.2, 022002 (2026).
- [3] F. S. Yu, H. Y. Jiang, R. H. Li, C. D. Lü, W. Wang and Z. X. Zhao, *Chin. Phys. C* **42**, 051001 (2018).
- [4] H. D. Politzer, *Phys. Rev. Lett.* **30**, 1346-1349 (1973).
- [5] D. J. Gross and F. Wilczek, *Phys. Rev. Lett.* **30**, 1343-1346 (1973).
- [6] H. J. Wang, P. R. Li, X. R. Lyu, J. Tandean and H. B. Li, *Sci. Bull.* **70**, no.8, 1183-1185 (2025).
- [7] M. Ablikim *et al.* (BESIII Collaboration), [arXiv:2508.11400 [hep-ex]]. [arXiv:2508.11400](https://arxiv.org/abs/2508.11400) [hep-ex].
- [8] H. Y. Cheng and B. Tseng, *Phys. Rev. D* **48**, 4188-4202 (1993).
- [9] J. G. Korner and M. Kramer, *Z. Phys. C* **55**, 659-670 (1992).
- [10] P. Zenczykowski, *Phys. Rev. D* **50**, 402-411 (1994).
- [11] P. Zenczykowski, *Phys. Rev. D* **50**, 5787-5792 (1994).
- [12] A. Datta, [arXiv:hep-ph/9504428](https://arxiv.org/abs/hep-ph/9504428) [hep-ph].
- [13] H. Y. Cheng and B. Tseng, *Phys. Rev. D* **55**, 1697 (1997).
- [14] M. A. Ivanov, J. G. Korner, V. E. Lyubovitskij and A. G. Rusetsky, *Phys. Rev. D* **57**, 5632-5652 (1998).
- [15] B. C. Ke, J. Koponen, H. B. Li and Y. Zheng, *Ann. Rev. Nucl. Part. Sci.* **73**, 285-314 (2023).
- [16] M. Ablikim *et al.* (BESIII Collaboration), *Nucl. Instrum. Meth. A* **614**, 345 (2010).
- [17] C. H. Yu *et al.*, *Proceedings of IPAC2016, Busan, Korea, 2016*.
- [18] M. Ablikim *et al.* (BESIII Collaboration), *Chin. Phys. C* **44**, 040001 (2020).
- [19] P. Cao, H. F. Chen, M. M. Chen, H. L. Dai, Y. K. Heng, X. L. Ji, X. S. Jiang, C. Li, X. Li and S. B. Liu, *et al. Nucl. Instrum. Meth. A* **953**, 163053 (2020) [doi:10.1016/j.nima.2019.163053](https://doi.org/10.1016/j.nima.2019.163053).
- [20] S. Agostinelli *et al.* (GEANT4 Collaboration), *Nucl. Instrum. Meth. A* **506**, 250 (2003).
- [21] S. Jadach, B. F. L. Ward and Z. Was, *Phys. Rev. D* **63**, 113009 (2001); *Comput. Phys. Commun.* **130**, 260 (2000).
- [22] D. J. Lange, *Nucl. Instrum. Meth. A* **462**, 152 (2001); R. G. Ping, *Chin. Phys. C* **32**, 599 (2008).
- [23] S. Navas *et al.* (Particle Data Group), *Phys. Rev. D* **110**, no.3, 030001 (2024).
- [24] J. C. Chen, G. S. Huang, X. R. Qi, D. H. Zhang and Y. S. Zhu, *Phys. Rev. D* **62**, 034003 (2000); R. L. Yang, R. G. Ping and H. Chen, *Chin. Phys. Lett.* **31**, 061301 (2014).
- [25] E. Barberio, B. van Eijk and Z. Was, *Comput. Phys. Commun.* **66**, 115 (1991).
- [26] J. P. Alexander *et al.* (CLEO Collaboration), *Phys. Rev. D* **53**, 1013-1017 (1996).
- [27] K. Abe *et al.* (Belle Collaboration), *Phys. Lett. B* **524**, 33-43 (2002).
- [28] M. Ablikim *et al.* (BESIII Collaboration), *Phys. Rev. Lett.* **117**, no.23, 232002 (2016).
- [29] R. Aaij *et al.* (LHCb Collaboration), *JHEP* **03**, 043 (2018).
- [30] R. Aaij *et al.* (LHCb Collaboration), *Phys. Rev. Lett.* **128**, no.6, 062001 (2022).
- [31] R. Aaij *et al.* (LHCb Collaboration), *Phys. Rev. Lett.* **131**, no.3, 031901 (2023).
- [32] H. Albrecht *et al.* (ARGUS Collaboration), *Phys. Lett. B* **241**, 278 (1990).
- [33] M. Pivk and F. R. Le Diberder, *Nucl. Instrum. Meth. A* **555**, 356-369 (2005).
- [34] S. U. Chung, CERN Academic Training Lecture, CERN Yellow Reports: Monographs, CERN-1971-008 (1971).
- [35] J. D. Richman, *Caltech Report CALT-68-1148*, California Institute of Technology, Pasadena, CA (1984).
- [36] Y. Jiang, *Nuovo Cim. C* **47**, no.4, 203 (2024).

- [37] S. U. Chung, *Phys. Rev. D* **57**, 431-442 (1998).
- [38] F. Von Hippel and C. Quigg, *Phys. Rev. D* **5**, 624-638 (1972).
- [39] M. Ablikim *et al.* (BESIII Collaboration), *Phys. Rev. Lett.* **131**, no.19, 191901 (2023).
- [40] M. Ablikim *et al.* (BESIII Collaboration), *JHEP* **12**, 033 (2022).
- [41] S. M. Flatte, *Phys. Lett. B* **63**, 224 (1976).
- [42] M. Ablikim *et al.* (BES Collaboration), *Phys. Lett. B* **607**, 243-253 (2005).
- [43] R. Aaij *et al.* (LHCb Collaboration), *Phys. Rev. Lett.* **115**, 072001 (2015).
- [44] C. Langenbruch, *Eur. Phys. J. C* **82**, 393 (2022).
- [45] M. Ablikim *et al.* (BESIII Collaboration), Measurements of the absolute branching fractions of the  $\Lambda_c^+$  hadronic decays, to be submitted to JHEP.
- [46] M. Ablikim *et al.* (BESIII Collaboration), *Phys. Rev. D* **101**, no.3, 032008 (2020).
- [47] M. Ablikim *et al.* (BESIII Collaboration), *Chin. Phys. C* **47**, no.2, 023001 (2023).